

Determining Conditions for the Fenton Reaction through Spectroscopy of FeSCN^{2+} and Methyl Orange

Nirbaan Maken¹ and Karel Villanueva[#]

¹West Windsor Plainsboro High School South

[#]Advisor

ABSTRACT

Exposure to radiation can lead to the breakdown of water into reactive oxygen species (ROS), such as hydroxyl radicals ($\text{OH}\cdot$), through a process called radiolysis. The presence of hydroxyl radicals ($\text{OH}\cdot$) and other ROS can cause mutations to DNA in the human body. While hydrogen peroxide (H_2O_2), a product of radiolysis, may not be a strong ROS on its own, it can react with certain metal ions such as iron(II) to produce hydroxyl radicals in a process called the Fenton reaction. This study investigates the optimal conditions for the Fenton reaction using a cost-effective spectroscopic analysis of ferric thiocyanate and degradation of methyl orange to detect the presence of Fe^{3+} and $\text{OH}\cdot$. Understanding conditions and methods of detection for the Fenton reaction is relevant due to the carcinogenic nature of the hydroxyl radicals produced (Kumar et al., 2021). The results of the spectroscopic analysis suggest that the Fenton reaction occurs ideally in acidic environments ($\text{p} = 0.00354$) with low temperature dependence. Additionally, both spectroscopic methods are effective for detecting the efficiency of Fenton processes. This study provides valuable insights for future research on the Fenton reaction and its potential applications.

Introduction

This study focuses on the optimal conditions for the Fenton reaction and the reliability of UV-Vis spectroscopy. The Fenton reaction is a reaction between ferrous ions and hydrogen peroxide that produces hydroxyl radicals, hydroxide ions, and ferric ions



In this study, experiments were performed involving the Fenton reaction with a goal of determining the optimal pH and temperature in which the most radicals were produced. This allows for a greater understanding of the extent to which this reaction occurs in human bodies and how the byproducts of radiolysis may interact with biological systems as illustrated below.

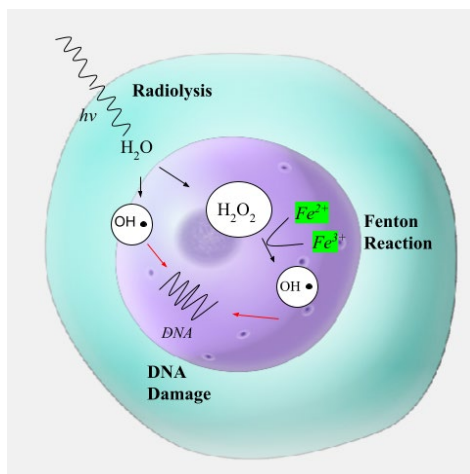


Figure 1. Representation of Fenton reaction's intracellular mechanism. The reaction is initiated under exposure to radiation where water decomposes into hydroxyl radicals and hydrogen peroxide. Hydrogen peroxide may further react with ferrous ions to significantly increase the concentration of radicals in the cell.

This study also aimed to determine the effectiveness of a novel, cost-effective spectroscopic method of detection for the Fenton reaction. Significant research has been done on the direct effect of radiation on DNA, yet there is limited research on the reactions between hydroxyl radicals and DNA that make up a substantial portion of mutations. This study incorporates a new method of determining the environment in which hydroxyl radicals are readily produced through the spectroscopy of ferric thiocyanate. Many other studies take advantage of NMR spectroscopy to directly measure the concentrations of radicals produced which can be costly and limited. One of the biggest disadvantages of the Fenton reaction is high cost (Xu et al., 2020) and using UV-Vis spectroscopy will allow for the study of the production of hydroxyl radicals to be more widespread and cost-effective. This is pivotal for future study in how these lead to the development of cancer and determine methods of regulating these radicals for patients who undergo radiotherapy.

The study of the Fenton reaction is important due to the carcinogenic character of its products. The hydroxyl radicals produced as a result of radiolysis and the Fenton reaction have the ability to oxidize and damage DNA as shown in Figure 1. The reaction between guanine and hydroxyl radicals, for example, produce 8-oxoguanine - a mutated base. 8-oxoguanine can then lead to transversion mutations where the base guanine (G) is converted to thymine (T) (Nakabeppu, 2014).

In the Fenton reaction, iron(II) is oxidized to iron(III). Ferric ions can form complexes that absorb light in the visible spectrum, allowing for the usage of UV-Vis spectroscopy to determine absorbance (A) of these compounds. This spectroscopic process was tested as a cost-efficient means of determining the extent of oxidation for iron in the Fenton reaction.

The degradation of methyl orange (MO) served as a secondary measure of determining the extent of the Fenton reaction through visible spectroscopy. To detect the presence of hydroxyl radicals, MO was added to the solution and its absorbance was measured over time. MO rapidly reacts with hydroxyl radicals to form organic acids (Butt et al., 2021). Though MO is not a DNA base, its degradation demonstrates the reactivity of hydroxyl radicals in the presence of organic molecules.

While the results of the two spectroscopic methods used in this study should theoretically be the same, the products of the Fenton reaction differ in the conditions in which they are produced due to the interference of various side reactions.

Materials & Equipment

All the materials were purchased from Flinn Scientific Inc. The chemicals used are as follows: 5 mM (4.990 mM) FeSO_4 prepared with 0.3475 g solid iron(II) sulfate hydrate, 0.1000 M H_2SO_4 stock solution, 5 mM (5.001 mM) KSCN prepared with 0.2430 g solid potassium thiocyanate, 0.0932 M KMnO_4 , 0.1000 M $\text{C}_2\text{H}_2\text{O}_4$ prepared with 1.2600 g hydrated $\text{C}_2\text{H}_2\text{O}_4$ solid, 0.1995 M $\text{Fe}(\text{NO}_3)_3$ prepared with 0.8060 g solid iron(III) nitrate nonahydrate, and 0.030 M H_2O_2 prepared with 30% hydrogen peroxide.

Solutions of FeSO_4 , KSCN, $\text{Fe}(\text{NO}_3)_3$, KMnO_4 , and $\text{C}_2\text{H}_2\text{O}_4$ were prepared using 250.0 mL volumetric flasks. The potassium permanganate solution was vacuum filtered in order to remove any insoluble KMnO_4 . Since concentration was not tested as an independent variable, the same solutions were used throughout the experiments. Ideal concentrations for the Fenton reaction were determined through previous research by Abdur-Rahim A. Giwa (Giwa et al., 2020).

Standardization of Potassium Permanganate

In order to determine the concentration for hydrogen peroxide, H_2O_2 must be titrated with a solution of KMnO_4 . Additionally, the concentration of the potassium permanganate solution must be precisely determined by standardizing with oxalic acid. 10.00 mL of 0.1000 M $\text{C}_2\text{H}_2\text{O}_4$ was placed in a beaker, along with 8.00 mL of 0.1000 M sulfuric acid. A burette was rinsed with distilled water and potassium permanganate, and then filled with the potassium permanganate solution. The oxalic acid was then titrated using a procedure developed by Mehraj Mahmud (Mahmmud, n.d.). The final permanganate concentration was determined to be 0.0932 M.

Standardization of Hydrogen Peroxide

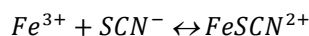
Since hydrogen peroxide decomposes into oxygen gas and water (Pędziwiatr et al., 2018), the solution of H_2O_2 was standardized with 0.0932 M potassium permanganate. 10.00 mL of Hydrogen Peroxide (Unknown Concentration), 10.00 mL of 0.1000 M sulfuric acid, and 10.00 mL of distilled water were added to a beaker. A burette was first rinsed with distilled water and potassium permanganate, then filled with the standardized 0.0932 M KMnO_4 . The acidified hydrogen peroxide solution was then titrated with the potassium permanganate and the concentration of hydrogen peroxide was determined to be 0.0960 M. This was then diluted to a final concentration of 0.0300 M H_2O_2 .

Methods

The concentration of Fe^{3+} was measured to determine the extent to which the Fenton reaction occurred. Ferric ions achieve maximum absorption at wavelengths between 300 and 305 nm (Yahia, 2016), but it complexes with SCN^- , producing FeSCN^{2+} . The ferric thiocyanate complex absorbs strongly in the visible range, allowing the use of cost-efficient and readily available Vernier Spectrophotometers to characterize the absorption spectrum. By adding an excess of Potassium Thiocyanate, KSCN, virtually all of the ferric ions in solutions form ferric thiocyanate. Then, the concentration of Fe^{3+} produced by the Fenton reaction can be determined by referencing a calibration curve.

To determine this calibration curve, solutions of 2.000 mM KSCN and 0.1995 (~0.2) M $\text{Fe}(\text{NO}_3)_3$ were prepared with the initial materials. First, 1.00 mL of the $\text{Fe}(\text{NO}_3)_3$ and 2.00 mL of the KSCN solution were mixed and diluted in a 10.00 mL volumetric flask. The cuvette was placed into a Vernier Spectrophotometer (Go Direct® SpectroVis® Plus Spectrophotometer) and absorbance was plotted against wavelength. The wavelength of maximum absorbance was determined to be 446.8 nm and would function as a reference to compare the absorbance values of varying concentrations of the ferric thiocyanate solutions. Four more solutions were prepared using varying concentrations of KSCN and were placed in the spectrophotometer. The absorbance values of these solutions at a wavelength

of 446.8 nm were measured and recorded. The final concentration of FeSCN^{2+} was assumed to be equal to the initial concentration of KSCN since the large excess of $\text{Fe}(\text{NO}_3)_3$ allows for the complexation reaction to essentially go to completion, removing all of the SCN^- .



The absorbance values of varying concentrations of FeSCN^{2+} at a wavelength of 446.8 nm were recorded (Table 1) and were plotted in Vernier Data Analysis. Linear regression was performed to create the curve (Graph 1).

Table 1. Data table of volumes of iron(III) Nitrate and KSCN added to the reaction mixture. Concentrations of FeSCN^{2+} listed above are equal to the concentrations of SCN^- in the reaction mixture. The maximum absorbance was taken at 446.8 nm from Vernier Spectral Analysis.

Volume of iron(III) Nitrate (mL)	Volume of Potassium Thiocyanate (mL)	Concentration of FeSCN^{2+} (M)	Maximum A at wavelength of 446.8 nm
1.00 mL $\text{Fe}(\text{NO}_3)_3$	3.50 mL KSCN	0.000700	1.994
1.00 mL $\text{Fe}(\text{NO}_3)_3$	2.50 mL KSCN	0.000500	1.346
1.00 mL $\text{Fe}(\text{NO}_3)_3$	1.50 mL KSCN	0.000300	1.063
1.00 mL $\text{Fe}(\text{NO}_3)_3$	0.50 mL KSCN	0.000100	0.518

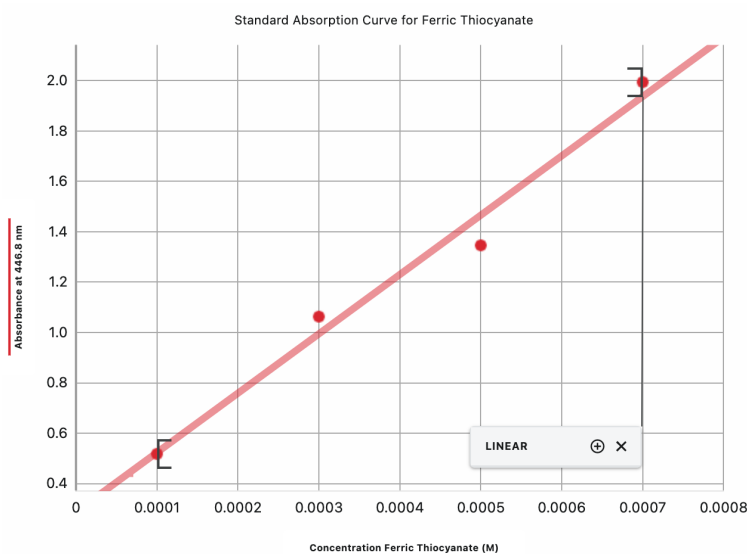


Figure 2. Calibration curve for ferric thiocyanate. Four different solutions of FeSCN^{2+} with varying concentrations were prepared and their absorbance at 446.8 nm was tested using a Vernier Spectrophotometer and plotted in Vernier Spectral Analysis. Linear regression was applied. Linear regression equation: $y = 2356x + 0.288$. Standard Deviation = 0.614. CV (Coefficient of Variation) < 1. Statistics obtained through Vernier Linear Regression Statistics.

Fenton Reaction

The Fenton reaction was tested under various pH and temperature conditions, and the absorbance curve of ferric thiocyanate after each trial was determined. This was done to determine the conditions in which Fe^{2+} is most easily oxidized and the Fenton reaction occurs. Procedures and ideal times for the Fenton reaction were developed through previous research by Andrea Y. Satoh (Satoh et al., 2007). After the reaction occurred, the products were mixed with KSCN in order for the iron(III) ions produced in the reaction to complex with the thiocyanate to form FeSCN^{2+} . The absorption curve was determined through spectrophotometry and compared to the standard curve (Figure 1) to determine the concentration of iron(III) produced.

25.00 mL of distilled water was added to a beaker, along with 5.00 mL of 5.000 mM FeSO_4 . The pH was adjusted using H_2SO_4 and measured with a Vernier pH Sensor. The solution was placed on a hot plate, the temperature was adjusted, and the reaction was initiated with the addition of 5.00 mL of 30.00 mM H_2O_2 . After 10 minutes, the Vernier spectrophotometer was calibrated with the reaction mixture prior to adding SCN^- , in order to eliminate the effects of absorption of extraneous species on the measurement. Then, 1.00 mL of 0.2000 M KSCN and 9.00 mL of the reaction mixture were added to a beaker. After mixing, they were placed in the spectrophotometer and the absorbance spectrum was obtained.

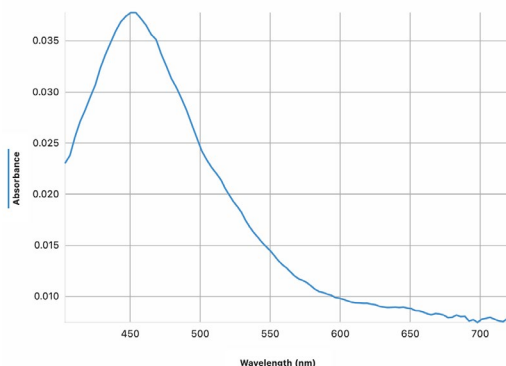


Figure 3. Example of absorbance vs wavelength for ferric thiocyanate at a pH of 5.0. Created 10 minutes after reaction was initiated and iron(III) was mixed with excess KSCN. Graph was taken from Vernier Spectral Analysis.

This graph had a peak at approximately 450 nm, which is consistent with the peak observed during the determination of the ferric thiocyanate standard calibration curve. As stated before, the spectrophotometer was calibrated with the reaction mixture which eliminates absorbance readings of substances. Thus, by mixing the KSCN with the reaction mixture and measuring the absorbance of the new solution, the spectrum would only correspond to the absorbance of newly produced species. The peak at approximately 450 nm demonstrates that FeSCN^{2+} was being produced and the oxidation of iron(II) through the Fenton Process was occurring, since iron(III) ions were available to complex with thiocyanate ions.

Seven different pH values were tested in this experiment. These values, along with a picture of the absorbance spectrum of a single trial, are represented below.

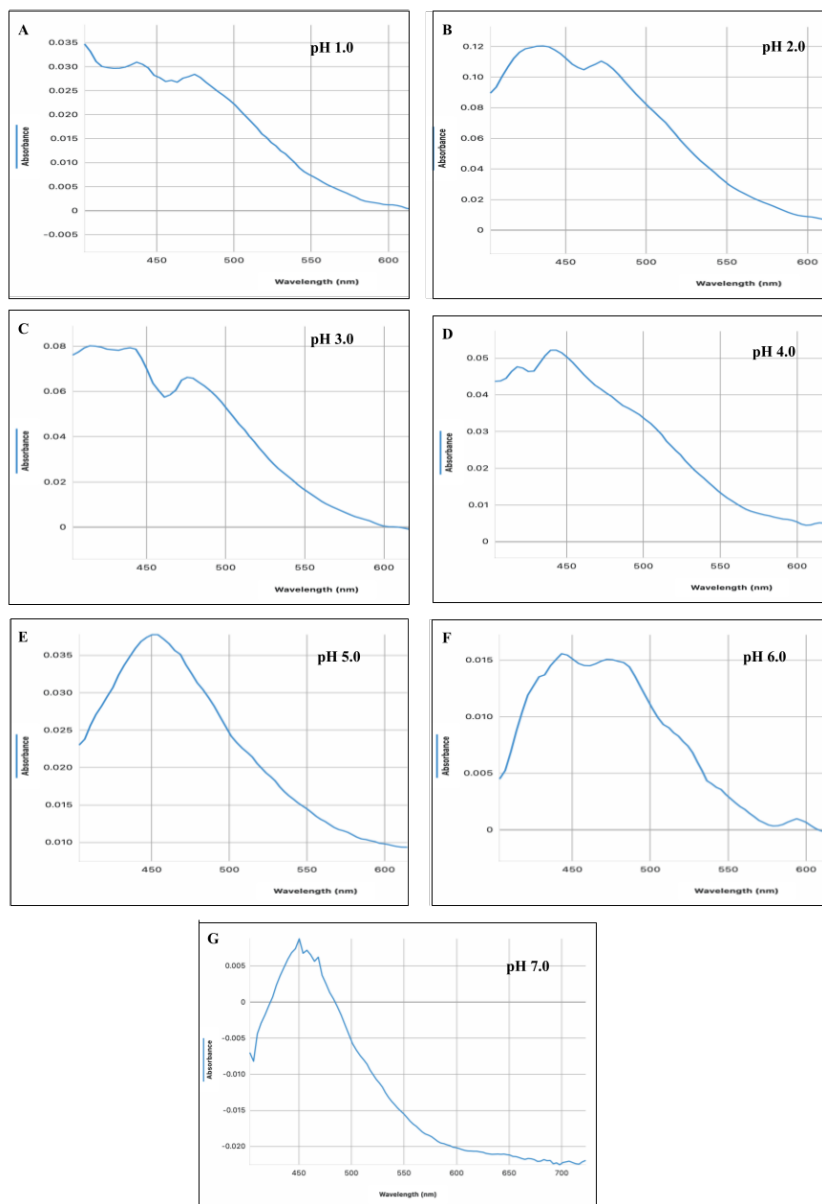


Figure 4. Absorbance spectra for one trial at each measured pH. Spectrums were taken from Vernier Spectral Analysis after 10 minutes of the Fenton reaction and addition of KSCN to the solution. Magnitude of absorbance is demonstrated on the x-axis.

Average Concentration of Fe^{3+} in Different pH Conditions

Each pH was tested for 3 trials and absorbance values at 446.8 nm from each trial were averaged. From here, the absorbance values were converted to concentrations using the standard absorbance curve (Figure 1).

Table 2. Data table of average absorbance for FeSCN^{2+} and calculated concentration of Fe^{3+} under various pH conditions.

pH	Average A	Average Concentration Fe^{3+}
1.0	0.028	0.0000054
2.0	0.115	0.0000222
3.0	0.095	0.000018
4.0	0.051	0.0000098
5.0	0.042	0.0000081
6.0	0.015	0.0000029
7.0	0.005	0.000001

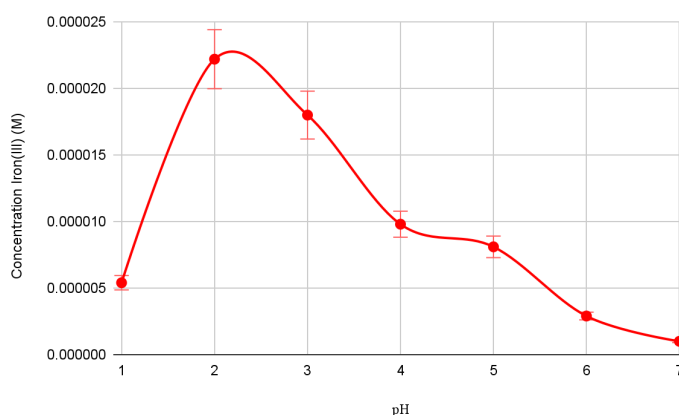
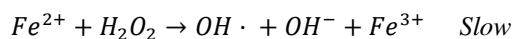


Figure 5. Concentration of iron(III) produced under different pH conditions (N=3). FeSCN^{2+} was produced upon the addition of KSCN in Fenton reaction systems in seven different pH environments. Absorbance of FeSCN^{2+} was converted to Fe^{3+} concentrations. Error bars present standard deviation. $P < 0.05$ ($P = 0.00354$) indicating significant dependence of iron(III) concentration on pH. Statistics obtained through a two tailed T-Test.

FeSCN^{2+} Absorbance Over Time

One of the ferric thiocyanate solutions at a pH of 3.0 was placed into the Vernier Spectrophotometer and its absorbance at a wavelength at 446.8 nm was measured over time. The two reactions occurring over time are represented below.



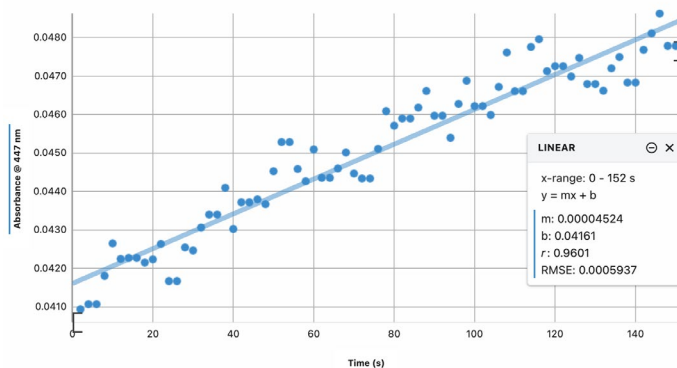


Figure 6. Absorbance over time for FeSCN^{2+} at pH 3.0. Ferric thiocyanate was placed in a cuvette absorbance and was measured at a wavelength of 446.8 nm over time. Linear Regression was applied. Standard Deviation = 0.002 and $m = 0.00004524$, indicating an increase in 0.00004524 units of absorbance each second.

In this graph, the absorbance of FeSCN^{2+} increases over time due to the progression of the Fenton reaction in solution. As the Fenton reaction proceeds, the Fe^{3+} concentration increases and reacts with the excess SCN^- that is present, thereby increasing the concentration and absorbance of ferric thiocyanate over time.

The rapid complexation of Fe^{3+} and SCN^- increases the applicability of this spectroscopic method of detection as changes in the concentration of FeSCN^{2+} will depend solely on the changes in concentration of Fe^{3+} , allowing for further potential research in the kinetics of the Fenton reaction.

Effect of Temperature on Concentration of Iron(III)

Three different temperatures, 25°C, 35°C, and 45°C were tested in this experiment. The concentration of iron(III) was determined using the same method. The pH was held constant at a value of 3.0, each temperature was tested for a total of 3 trials, the absorbance values of FeSCN^{2+} were converted to Fe^{3+} Concentrations, which were then averaged across all 3 trials.

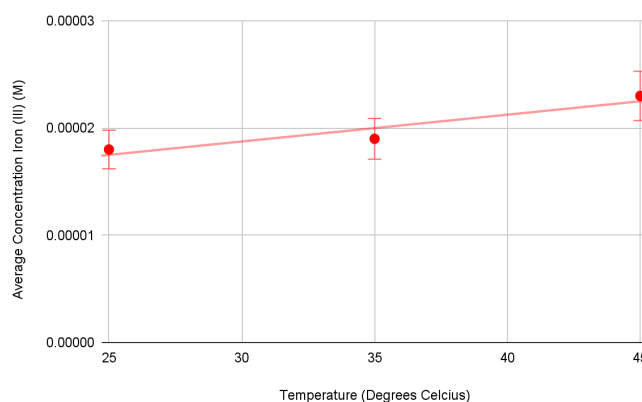


Figure 7. Average concentration of Fe^{3+} under different temperature conditions ($N = 3$). FeSCN^{2+} was produced upon the addition of KSCN in Fenton reaction systems in 3 different temperatures at a constant pH of 3.0. Absorbance of FeSCN^{2+} was converted to Fe^{3+} concentrations. Linear Regression was applied. $P < 0.05$ ($P = 0.00000100$) indicating significant dependence of iron(III) concentration on temperature. Statistics obtained through a one tailed T-Test.

Degradation of Methyl Orange

After the preparation of each solution from the initial procedure, methyl orange was added to the remaining reaction mixture and its absorbance at a specific wavelength was measured over time. These results were compared with the absorbance of the ferric thiocyanate to determine if the ideal conditions for the Fenton reaction were consistent between the two procedures.

After the absorbance of ferric thiocyanate in a certain mixture was determined, 3 drops of methyl orange were added, the solution was added to a cuvette, and absorbance was taken at the wavelength of maximum absorbance, 472.2 nm. After 35 minutes, the absorbance was measured at the same wavelength to determine the extent of degradation.

Both FeSO_4 and H_2O_2 were tested separately to determine if they contributed to the degradation of methyl orange. When tested, it was determined that both of these compounds did not change the absorbance values of methyl orange over the time span of 35 minutes, meaning the measurements accounted exclusively for the Fenton reaction products.

Figure 7 represents an example of the difference in absorbance spectrums for methyl orange after 35 minutes in the presence of $\text{OH}\cdot$ in a system with a pH of 3.0.

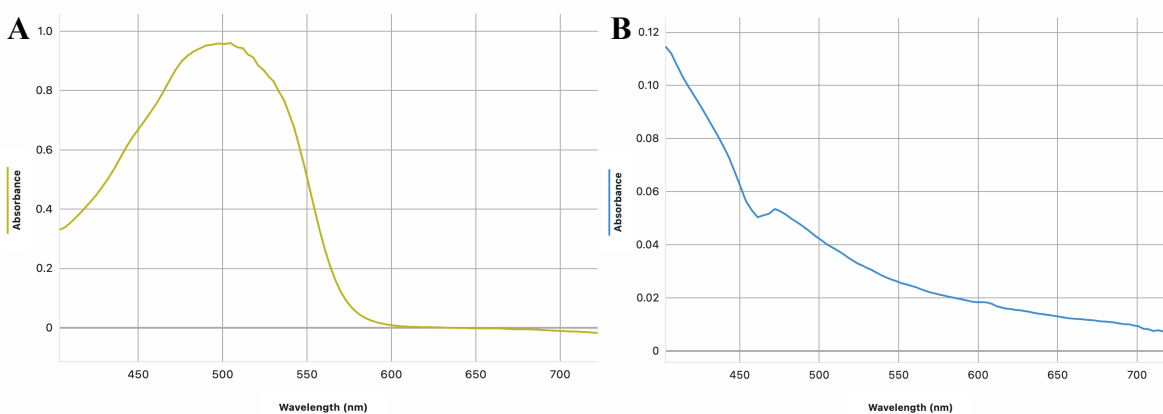


Figure 8. Graphs of absorbance vs wavelength taken in Vernier Spectral Analysis. Graph **A** represents initial absorbance of MO, while Graph **B** represents absorbance after 35 minutes in the Fenton reaction system.

Initially, the absorbance value at 472.2 nm is very high (0.870) and the peak is well defined. However, after 35 minutes, the absorbance value at this wavelength drops to a much lower value (0.055) and the peak is no longer discernible. The difference in absorbance values is consistent with the fact that hydroxyl radicals are reacting with the dye, thereby decreasing MO's concentration and observed absorbance. Furthermore, the creation of an unclear peak is due to the production of hydrocarbons and other side products (CO_2 , H_2O) of the reaction. However, the small peak at 472.2 nm in the second graph demonstrates the presence of remaining methyl orange molecules.

Average Percent Degradation of Methyl Orange in Different pH Conditions

The degradation of methyl orange was tested under seven different pH conditions. The differences between the initial absorbance values and the values after 35 minutes were used to calculate the percent degradation. The process was repeated for two trials at each pH value. The two values from each trial were averaged to obtain the average percent degradation at each pH.

Table 3. Data table with average absorbance difference and percent degradation at various pH values for methyl orange.

pH	Average Percent Degradation (%)
1.0	0.90
2.0	77.7
3.0	93.9
4.0	77.2
5.0	73.0
6.0	65.9
7.0	30.8

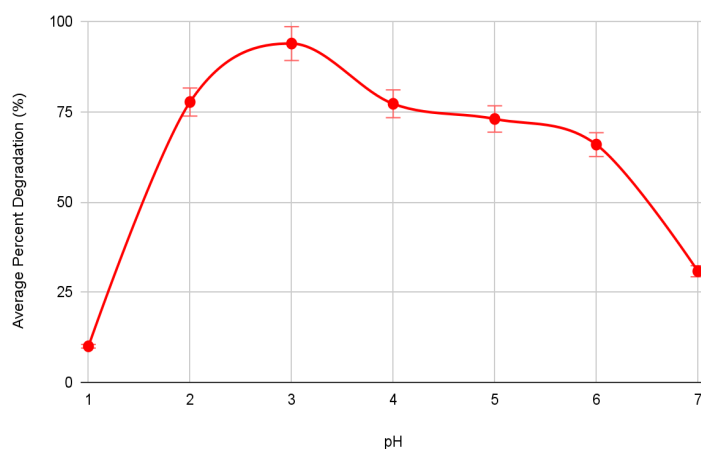


Figure 9. Percent degradation of methyl orange after 35 minutes under different pH conditions (N = 2). Final and initial absorbance values for methyl orange were measured using Vernier Spectral Analysis and the differences were converted to percent degradation. Error bars show standard deviation. $P < 0.05$ ($P = 0.00223$) indicating that the percent degradation of MO is significantly dependent on the pH. Statistics obtained through a two tailed T-Test.



Figure 10. A representation of two different reaction mixtures with the presence of methyl orange over time. Initially, when the dye is added, the solution turns bright orange. However, after 35 minutes, the hydroxyl radicals have reacted with the MO to form colorless hydrocarbons resulting in the production of a clearer solution shown on the right.

Results

Effect of pH

In the first experiment, a pH of 2.0 resulted in the highest production of iron(III) through the Fenton reaction (Figure 5). The Fe^{3+} concentration in this pH was 0.0222 mM after 10 minutes of the reaction. At a pH of 3.0, the concentration of Fe^{3+} was 0.018 mM (Table 2). At both a pH of 2.0, the highest concentrations of Fe^{3+} were produced, indicating that oxidation of iron(II) through the Fenton reaction is optimal under these conditions. At a pH lower than 2 and greater than 6, concentrations of iron(III) dropped significantly. This data corroborates previous research by Abdur-Rahim A. Giwa (Giwa et al., 2020).

This data is consistent with what occurred in the second experiment involving the degradation of methyl orange. As shown in Figure 9, the highest percent degradation occurred at a pH of 3.0 with a value of 93.9% followed by a degradation of 77.7% at a pH of 2.0. At a pH of 1.0, the percent degradation drastically drops to a value of 0.9%. A drop in percent degradation also occurred in pH values greater than 3 with an inverse relationship between pH and percent degradation. In this case, a pH 3.0 results in the highest production of hydroxyl radicals and execution of the Fenton reaction. These values are consistent with previous research done by Ge Song (Song et al., 2021) and Venkatarasimha Rao (Rao et al., 2016). These values are explained in the discussion section.

Effect of Temperature

Changing the temperature from 25°C to 35°C and 45°C had little effect on the concentration of iron(III) and the effectiveness of the Fenton reaction (Figure 7). The difference in concentrations of iron(III) produced from 25°C to 45°C was 0.0050 mM, resulting in a percent increase of 28% (Figure 7). This indicates that there is no significant increase that comes as a result of raising the temperature and the slight increase most likely stems from the increased rate of collision of reactants due to a higher kinetic energy in the 10 minute time frame. These results are consistent with previous research that indicates little change in efficiency of the Fenton reaction due to a temperature increase (Tengrui et al., 2007).

Spectroscopy of Ferric Thiocyanate vs. Methyl Orange

The spectroscopy of ferric thiocyanate served as a viable method of detection of ideal conditions for the Fenton processes. The oxidation of iron(II) to iron(III) was easily measured by adding in KSCN, to form ferric thiocyanate, a bright red molecule whose formation has a very high rate constant (Below et al., 1957). Due to the rapid formation of this complex, the concentration of Fe^{3+} produced from the Fenton reaction is able to be measured immediately through the use of the Vernier Spectrophotometer. However, to determine the conditions in which the most hydroxyl radicals produced, the second method of measuring the degradation of methyl orange was more effective. The organic dye was able to quickly degrade in the presence of these radicals in a time span of 35 minutes and the dye's bright orange color allowed for the use of visible light spectroscopy to measure degradation.

Discussion

Explanation for results

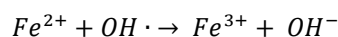
As shown in Figure 2, a pH range of 2.0 - 4.0 was determined to be a viable range for significant production of iron(III) through the Fenton reaction. A pH of 2.0 was determined to be ideal for the highest production of Fe^{3+} ions while a pH of 3.0 was determined to be ideal for the highest production of hydroxyl radicals. This discrepancy can be explained by the reaction between protons and hydroxyl radicals. In highly acidic solutions, these radicals are "scavenged" by hydrogen ions (Walling et al., 2021). This can explain the difference in optimal pH values between the two methods. In the spectroscopy of ferric thiocyanate, the most iron(III) ions were produced at a pH of 2.0 but the hydroxyl radicals in solution quickly reacted with the H^+ ions, reducing the concentration of the ROS. At a pH of 3.0, fewer Fe^{3+} ions were produced, but more radicals were retained in solution and able to degrade the methyl orange dye.

At a pH of less than 2.0, the Fenton reaction occurs to a very small extent due to the production of complex molecules such as $[Fe(H_2O)_6]^{2+}$ and $[H_3O_2]^+$ (Xu et al., 2020). At a pH greater than 4.0, there is significant production of ferric hydroxide precipitate. In acidic solution, Ferric Hydroxide becomes more soluble due to the presence of acid. In neutral and basic solution, however, iron(III) ions react with water to form ferric hydroxide and other iron hydroxides.

Difficulties and Limitations

The first issue arose when standardizing Hydrogen Peroxide with Potassium Permanganate. Potassium Permanganate tends to deteriorate after long periods of time (Rees, 1983). During the first titration of hydrogen peroxide, an unexpectedly large amount of $KMnO_4$ was needed to completely react with the peroxide. This can be explained by the deterioration of $KMnO_4$ and the resulting decrease in the concentration of the Potassium Permanganate solution over time. Thus, a new $KMnO_4$ solution was prepared and standardized with oxalic acid.

The limitations of this process arise from the presence of side reactions. Other fenton processes also result in the production of iron(III), (De Laat & Gallard, 1999).



Hydroxyl radicals attack ferrous ions, gaining an extra electron to form hydroxide ions while simultaneously oxidizing iron(II) to iron(III). Therefore, amounts of iron(III) may have been altered by the presence of these side reactions.

Further Potential Research

One specific way the methods in this study can be applied for future use in the field of cancer is determining the types of radiotherapy that lead to the highest production of hydroxyl radicals. In terms of using the degradation of methyl orange, separate solutions of water and MO can be prepared and treated with different types of radiation used in radiotherapy: x-rays, gamma rays, electron beams, and protons. The degradation of methyl orange, along with a subsequent comparison of absorbance spectrums, can be used as a method of determining the solutions in which the greatest amount of hydroxyl radicals were produced (Smith et al., 2021). Furthermore, separate solutions with FeSO_4 and water can be tested under the different types of radiation listed above. The water will break down into H_2O_2 which will further react with iron(II) to form hydroxyl radicals and iron(III). From there, the method of adding KSCN to form ferric thiocyanate and measuring its absorbance can allow for another determination of the type of radiation that initiates the Fenton reaction in the human body.

Observations

In reaction mixtures with a pH greater than 5.0, the solution became very cloudy and thick. This is consistent with the previous research by Andrea Y. Satoh (Satoh et al., 2007) and the observation that higher pH's lead to the creation of iron(III) hydroxide precipitate. At low concentrations, iron(III) hydroxide sludge is produced, resulting in an opaque yellow solution.



Fenton Reaction Implications/Applications

The reactivity of hydroxyl radicals can be seen as a double-edged sword. There are many deleterious effects of radicals on DNA that can lead to the development of tumors. On the other hand, this species' ability to attack organic molecules has been manipulated in order to remove harmful toxins and chemicals from certain substances.

One area where the Fenton reaction is used beneficially is the treatment of wastewater. Fenton reaction is often used to treat "oily wastewater" which is water that contains fats and greases (Ayoub, 2022). Hydroxyl radicals are able to degrade the organic pollutants and effectively remove the oils and other harmful molecules from the wastewater.

Furthermore, the radicals produced from the Fenton reaction also have beneficial applications in the field of cancer. Research by Chenyang Jia (Jia et al., 2021) demonstrates the use of "Chemodynamic" therapy where the Fenton reaction is initiated in a region where a tumor is present to attack cancerous cells. In this research paper, many numerous benefits of this new type of cancer therapy were discussed such as its selectivity towards the tumor itself. It was further demonstrated that this therapy can be coupled with other types of cancer therapy to maximize tumor

removal. Research by Xingyang Zhao (Zhao et al., 2022) has proven that the Fenton reaction is a viable method of damaging cancerous cells. Fe^{2+} in the cell reacts with the produced Hydrogen Peroxide under an “acidic microenvironment” due to the low pH requirements of the Fenton reaction shown in the results above.

Conclusion

The Fenton reaction is of great interest due the production of hydroxyl radicals, a highly reactive species. Under exposure to radiation, hydrogen peroxide in biological systems can form radicals by reaction with Fe^{2+} ions. In this experiment and previous research, it was determined that this reaction is ideal under acidic conditions (pH of 2-4) but still occurs to some extent under physiological conditions. It was also determined that visible light spectroscopy of ferric thiocyanate and methyl orange serves as a viable method for determining the extent of the Fenton reaction and activity of its products. The degradation of methyl orange served as a more effective method of radical detection while the ferric thiocyanate method proved to have broader applicability in the kinetic study of the reaction. Understanding methods of production for these hydroxyl radicals is pivotal due to the numerous potential applications of these reactive radicals for research purposes in the fields of cancer and wastewater treatment.

Acknowledgements

I would like to express my deep gratitude for Karel Villanueva (Kean University) for providing equipment, supervising projects, and assisting with experimental procedures. I also would like to thank Cynthia Jaworsky for assisting with experimental procedures and providing necessary chemicals. Finally, I would like to thank WWP District Supervisor Richard Stec and District Superintendent David Aderhold for providing permission to proceed with the research project.

Funding Acknowledgement

The author received no financial support for the research, authorship, and/or publication of this article.

Competing Interest

The author declares that there is no conflict of interest.

Data Availability

All data generated or analyzed during this study are included in this published article (and its Supplementary Information files). The paper and supplementary data is also available on ChemRxiv as a preprint (DOI: 10.26434/chemrxiv-2023-8w46q).

References

Kumar, P., Pottiboyina, S., & Sevilla, M. (2011). Hydroxyl radical ($\text{OH}\bullet$) reaction with guanine in an aqueous environment: a DFT study. *Journal of Physical Chemistry A*, 115(49), 13065-13072. doi:10.1021/jp208841q

- Giwa, A. R. A., Bello, I. A., Olabintan, A. B., Bello, O. S., & Saleh, T. A. (2020). Kinetic and thermodynamic studies of fenton oxidative decolorization of methylene blue. *Heliyon*, 6(8), e04454. doi:10.1016/j.heliyon.2020.e04454
- Xu, M., Wu, C., & Zhou, Y. (2020). Advancements in the Fenton process for wastewater treatment. *IntechOpen*. doi:10.5772/intechopen.90256
- Cerchiaro, G., Bolin, C., & Cardozo-Pelaez, F. (n.d.). Hydroxyl radical oxidation of guanosine 5'-triphosphate (GTP): requirement for a GTP-Cu(II) complex. *Redox Biology*, 14, 101506. doi:10.1016/j.redox.2019.101506
- Chiorcea-Paquim, A. M. (2022). 8-oxoguanine and 8-oxodeoxyguanosine Biomarkers of Oxidative DNA Damage: A Review on HPLC–ECD Determination. *Molecules*, 27(5), 1620. doi:10.3390/molecules27051620
- Nakabeppu, Y. (2014). Cellular Levels of 8-Oxoguanine in either DNA or the Nucleotide Pool Play Pivotal Roles in Carcinogenesis and Survival of Cancer Cells. *International Journal of Molecular Sciences*, 15(7), 12543. doi:10.3390/ijms150712543
- Janik, B., Bartels, L., & Jonah, C. (2007). Hydroxyl radical self-recombination reaction and absorption spectrum in water up to 350 degrees C. *Journal of Physical Chemistry A*, 111(18), 5073-5079. doi:10.1021/jp065992v
- Yahia, L., & Yahia, C. (2007). Competition of Fe³⁺ UV-Vis Absorption between Ascorbic Acid (AA) and Clofibrilic Acid (CA). *Electronic Journal of Biology*, 3(3), 229-234. doi:10.1080/17479070701642223
- Hua, Y., Wang, Y., Kang, X., Xu, F., Han, Z., Zhang, C., Wang, Z. Y., Liu, J. Q., Zhao, X., Chen, X., & Zang, S. Q. (2021). A multifunctional AIE gold cluster-based theranostic system: tumor-targeted imaging and Fenton reaction-assisted enhanced radiotherapy. *Journal of Nanobiotechnology*, 19(1), 119. doi:10.1186/s12951-021-01191-x
- Zhao, X., Sun, X., Huang, W., Chen, R., Chen, K., Nie, L., & Fang, C. (2022). A microenvironment-responsive FePt probes for imaging-guided Fenton-enhanced radiotherapy of hepatocellular carcinoma. *Journal of Nanobiotechnology*, 20(1), 130. doi:10.1186/s12951-022-01305-z
- Jia, C., Guo, Y., & Wu, F. (2021). Chemodynamic Therapy via Fenton and Fenton-Like Nanomaterials: Strategies and Recent Advances. *Small*, 18(6), 2103868. doi:10.1002/sml.202103868
- Rees, G. (1983). The Stability of Potassium Permanganate Solutions. *Journal of Chemical Education*, 60(1), 60. doi:10.1021/ed060p60
- Janik, B., Bartels, L., & Jonah, C. (2007, March 15). Hydroxyl radical self-recombination reaction and absorption spectrum in water up to 350 degrees C. *Journal of Physical Chemistry A*, 111(18), 5073-5079. doi:10.1021/jp065992v
- Yahia, L., & Yahia, C. (2007, November 16). Competition of Fe³⁺ UV-Vis Absorption between Ascorbic Acid (AA) and Clofibrilic Acid (CA). *Electronic Journal of Biology*, 3(3), 229-234. doi:10.1080/17479070701642223
- Effect of Fenton-like reactions on the degradation of thiocyanate in water treatment. (2014, August 13). *Journal of Environmental Chemical Engineering*, 2(4), 1746-1754. doi:10.1016/j.jece.2014.08.010

- Barron, M. (2016, July 13). 4.4: UV-Visible Spectroscopy. Chemistry LibreTexts. Retrieved March 28, 2023, from [https://chem.libretexts.org/Bookshelves/Analytical_Chemistry/Physical_Methods_in_Chemistry_and_Nano_Science_\(Barron\)/04%3A_Chemical_Speciation/4.04%3A_UV-Visible_Spectroscopy](https://chem.libretexts.org/Bookshelves/Analytical_Chemistry/Physical_Methods_in_Chemistry_and_Nano_Science_(Barron)/04%3A_Chemical_Speciation/4.04%3A_UV-Visible_Spectroscopy)
- Satoh, T., Trosko, J. E., & Masten, S. J. (2007, March 15). Methylene Blue Dye Test for Rapid Qualitative Detection of Hydroxyl Radicals Formed in a Fenton's Reaction Aqueous Solution. *Environmental Science & Technology*, 41(7), 2878-2883. doi:10.1021/es0617800
- Song, G., Zhou, M., Du, X., Su, P., & Guo, J. (2021, June 2). Mechanistic Insight into the Heterogeneous Electro-Fenton/Sulfite Process for Ultraefficient Degradation of Pollutants over a Wide pH Range. *ACS ES&T Water*, 1(7), 1637-1647. doi:10.1021/acsestwater.1c00123
- Rao, C. V., Giri, A. S., Goud, V. V., & Golder, A. K. (2015, November 7). Studies on pH-dependent color variation and decomposition mechanism of Brilliant Green dye in Fenton reaction. *International Journal of Industrial Chemistry*, 7(1), 71-80. doi:10.1007/s40090-015-0060-x
- Tengrui, L., Al-Harbawi, A., Jun, Z., & Bo, L. M. (n.d.). The Effect and its Influence Factors of the Fenton Process on the Old Landfill Leachate. *Science Alert*. Retrieved March 28, 2023, from <https://scialert.net/fulltext/?doi=jas.2007.724.727>
- Below, F. E., & Connick, R. E. (1958, June 20). Kinetics of the Formation of the ferric thiocyanate Complex. *Journal of the American Chemical Society*, 80(12), 2961-2966. doi:10.1021/ja01276a042
- Walling, S. A., Um, W., Corkhill, C. L., & Hyatt, N. C. (2021, September 24). Fenton and Fenton-like wet oxidation for degradation and destruction of organic radioactive wastes. *npj Materials Degradation*, 5(1), 10. doi:10.1038/s41529-021-00192-3
- Smith, R. D., Pimblott, S. J., & LaVerne, J. A. (2021, June 9). Hydroxyl radical yields in the heavy ion radiolysis of water. *Radiation Physics and Chemistry*, 170, 109629. doi:10.1016/j.radphyschem.2021.109629
- Hirakawa, K. (2017, December 20). Biomolecules Oxidation by Hydrogen Peroxide and Singlet Oxygen. *IntechOpen*. doi:10.5772/intechopen.71465
- Privett, G. J., Teixeira, M. L., & Morales, F. J. (2017, April 4). Exploring water radiolysis in proton cancer therapy: Time-dependent, non-adiabatic simulations of H⁺ + (H₂O)₁₋₆. *PLOS ONE*, 12(4), e0174456. doi:10.1371/journal.pone.0174456
- Lousada, J., & Alonso, M. (2018, September 27). Fenton oxidation: A powerful tool for environmental remediation. *Environmental Science & Pollution Research*, 25(28), 22711-22727. doi:10.1007/s11356-018-1930-9
- Mahmmud, M. U. (n.d.). Standardization of Potassium Permanganate (KMnO₄) solution with standard Sodium Oxalate solution.docx. Retrieved from https://www.academia.edu/38424688/Standardization_of_Potassium_Permanganate_KMnO4_solution_with_standard_Sodium_Oxalate_solution.docx

Pędziwiatr, P., Mikołajczyk, F., Zawadzki, D., Mikołajczyk, K., & Bedka, A. (2018). Decomposition of hydrogen peroxide—kinetics and review of chosen catalysts. *Acta Innovations*, 26(1), 45-52. Retrieved from https://www.proakademia.eu/gfx/baza_wiedzy/461/nr_26_45-52_2_2.pdf

Butt, A. L., Mpinga, J. K., & Tichapondwa, S. M. (2021). Photo-Fenton oxidation of methyl orange dye using South African ilmenite sands as a catalyst. *Catalysts*, 11(12), 1452. doi:10.3390/catal11121452

De Laat, J., & Gallard, H. (1999). Catalytic decomposition of hydrogen peroxide by Fe(III) in homogeneous aqueous solution: mechanism and kinetic modeling. *Environmental Science & Technology*, 33(16), 2726-2732. doi:10.1021/es981171v

Ayoub, M. (2022). Fenton process for the treatment of wastewater effluent from the edible oil industry. *Water Science & Technology*, 85(12), 2905-2912. doi:10.2166/wst.2022.